NASA MEMO 12-29-58A

NASA

MEMORANDUM

EFFECTS OF LARGE WING-TIP MASSES ON OSCILLATORY STABILITY OF WING BENDING COUPLED WITH AIRPLANE PITCH

By Donald T. Higdon

Ames Research Center
Moffett Field, Calif.

NATIONAL AERONAUTICS AND SPACE ADMINISTRATION

WASHINGTON

January 1959

NATIONAL AERONAUTICS AND SPACE ADMINISTRATION

MEMORANDUM 12-29-58A

EFFECTS OF LARGE WING-TIP MASSES ON OSCILLATORY STABILITY OF WING BENDING COUPLED WITH AIRPLANE PITCH

By Donald T. Higdon

SUMMARY

An examination of oscillatory stability for a straight-winged airplane with large concentrated wing-tip masses was made using wing-bending and airplane-pitching degrees of freedom and considering only quasi-steady aerodynamic forces. It was found that instability caused by coupling of airplane pitching and wing bending occurred for large ratios of effective wing-tip mass to total airplane mass and for coupled wing-bending frequencies near or below the uncoupled pitching frequency. Boundaries for this instability are given in terms of two quantities: (1) the ratio of effective tip mass to airplane mass, which can be estimated, and (2) the ratio of the coupled bending frequency to the uncoupled pitch frequency, which can be measured in flight. These boundaries are presented for various values of several airplane parameters.

INTRODUCTION

The placement of fuel or armament in wing-tip pods is a practice which has been in existence for some time on fighter-type aircraft, and there are several ways in which large concentrated masses might appear at the wing tips of future aircraft. There is the possibility that in nuclear powered aircraft, where the personnel and power plant must be well separated, this technique will be employed. Long range aircraft with supersonic dash capability might carry disposable wing-tip sections with large fuel tanks. Also the mounting of engines at the wing tips is proposed for certain airplane types such as vertical take-off airplanes.

The natural wing-bending frequency of an airplane might be lowered by the presence of large wing-tip masses to the extent that it is near or even below the natural pitching frequency of the airplane under certain flight conditions. Under these conditions the effects of coupling between pitching and wing bending are of concern, since the damping ratios of structural modes are inherently low and any unfavorable coupling might cause oscillatory instability in coupled wing bending. It is the purpose of this study to establish conditions under which such wing-bending instability is likely to occur.

The analysis is made by means of equations of motion with airplane pitch and fundamental wing-bending degrees of freedom. Unsteady aerodynamics, that is, the effect of frequency on aerodynamic coefficients, and structural damping are neglected.

NOTATION

D derivative with respect to real time, $\frac{d}{dt}$

I airplane pitching moment of inertia about the center of gravity, slug ft^2

M total airplane mass, slugs

M_θ rate of change of pitching moment with pitch angle, θ, $-2\int_0^1 l_\theta x_{ac} d\eta$, ft-lb/radian

$M_{\dot\theta}$ rate of change of pitching moment with pitch velocity, $\dot\theta$, ft-lb sec/radian

Q_1 generalized aerodynamic pitching moment, ft-lb

Q_2 generalized aerodynamic wing-bending force, lb

S wing area, sq ft

V forward velocity of airplane, ft/sec

Y_{a_o} rate of change with the angle $\frac{\dot y}{V}$ of the generalized wing-bending force due to an angle-of-attack distribution $\frac{\dot y}{V} a_o(\eta)$, $2\int_0^1 l_{a_o} a_o d\eta$, lb/radian

Y'_{a_o} $\frac{Y_{a_o}}{Z_\theta}$

Y_θ rate of change of generalized wing-bending force with pitch angle θ, $2\int_0^1 l_\theta a_o d\eta$, lb/radian

Y'_θ $\frac{Y_\theta}{Z_\theta}$

Z_{a_o} rate of change with the angle $\frac{\dot{y}}{V}$ of the generalized vertical force due to an angle-of-attack distribution $\frac{\dot{y}}{V} a_o(\eta)$, $2\int_o^1 l_{a_o} d\eta$, lb/radian

Z'_{a_o} $\frac{Z_{a_o}}{Z_\theta}$

Z_θ rate of change of generalized vertical force or lift with pitch angle θ, $2\int_o^1 l_\theta d\eta$, lb/radian

$a(\eta)$ spanwise bending deflection as a function of η referenced to node and normalized on cantilever wing-tip deflection y

$a_o(\eta)$ spanwise bending deflection as a function of η referenced to wing root and normalized on cantilever wing-tip deflection y, $a(\eta) - a(0)$

$a(0)$ value of $a(\eta)$ at $\eta = 0$ or the wing root

$\bar{c}$ mean aerodynamic chord

e Naperian base

i $\sqrt{-1}$

k_θ reduced pitching frequency parameter, $\frac{\omega_\theta r}{V}$

l_a rate of change with the angle $\frac{\dot{y}}{V}$ of the spanwise aerodynamic load distribution due to an angle-of-attack distribution $\frac{\dot{y}}{V} a(\eta)$, lb/radian

l_{a_o} rate of change with the angle $\frac{\dot{y}}{V}$ of the spanwise aerodynamic load distribution due to an angle-of-attack distribution $\frac{\dot{y}}{V} a_o(\eta)$, lb/radian

l_θ rate of change with θ of the spanwise aerodynamic load distribution due to a pitch angle θ, lb/radian

m effective wing-tip mass (both tips), $2\int_0^1 \mu a_0 d\eta$, slugs

m' $\frac{m}{M}$

m_g generalized wing-bending mass, $2\int_0^1 \mu a^2 d\eta$, slugs

m_g' $\frac{m_g}{M}$

p derivative with respect to dimensionless time, $\frac{d}{d\tau}$

q dynamic pressure, lb/sq ft

r pitching radius of gyration $\sqrt{\frac{I}{M}}$, ft

$s(\eta)$ spanwise distribution of static mass moment about airplane center of gravity, slug ft

t real time, sec

u static margin, $\frac{M_\theta}{Z_\theta}$, ft

u' $\frac{u}{r}$

x longitudinal distance from airplane center of gravity, positive forward, ft

x_{ac} wing-fuselage local aerodynamic center relative to airplane center of gravity, positive forward

x_a wing local aerodynamic center relative to airplane center of gravity, positive forward

x_a' $\frac{x_a}{r}$

x_p longitudinal tip mass center of gravity relative to airplane center of gravity, positive forward, ft

x_p' $\frac{x_p}{r}$

y wing-tip deflection relative to wing root (cantilever), positive down, ft

ζ_B damping ratio of coupled wing-bending mode

ζ_y damping ratio of uncoupled, free-free, wing-bending mode

ζ_θ damping ratio of uncoupled pitching mode

η dimensionless spanwise station

θ pitch coordinate, positive nose up, radian

$\theta_{\dot{y}}$ component of pitch in phase with bending velocity during undamped oscillation

$\mu(\eta)$ spanwise mass distribution of airplane, slugs

τ dimensionless time, $\omega_\theta t$

Ω $\frac{\omega_B}{\omega_\theta}$

ω_B undamped natural frequency of coupled wing-bending mode, radians/sec

ω_y undamped natural frequency of uncoupled, free-free, wing-bending mode, radians/sec

ω_θ undamped natural frequency of uncoupled pitching mode, $\sqrt{-\frac{M_\theta}{I}}$, radians/sec

Dots over symbols are used to indicate differentiation with respect to real time.

DERIVATION OF EQUATIONS OF MOTION

Selection of Degrees of Freedom

A system with two degrees of freedom is considered for the purpose of studying oscillatory instability caused by coupling of wing bending with airplane-pitching motion. The selection of the two degrees of freedom was based on the results of some four degree of freedom studies on specific example airplanes, where the degrees of freedom were airplane pitch, airplane vertical translation, cantilever wing bending, and cantilever wing torsion. The examples were similar in character to the type of airplane considered in the present analysis. The development of the

equations was by the method shown in appendix C of reference 1. In these studies conditions of undamped oscillation in modes which were primarily wing bending were found and the modes of oscillation were examined.

Two important facts were noticed:

1. The relation between vertical translation and cantilever wing bending was nearly the same as would be expected for the airplane in an uncoupled, free-free, wing fundamental bending mode (in vacuo).

2. The role of wing torsion in reducing the generalized coupled mode damping force to zero was found to be small in comparison with the role of pitch, and instability could be achieved without the inclusion of the torsion degree of freedom under conditions not greatly different than with it.

The above observations indicated that the essential mechanism involved in this oscillatory instability could be preserved in a system of only two degrees of freedom, airplane pitch and a wing-bending degree of freedom based on the uncoupled, free-free, wing first-bending mode in the absence of aerodynamic forces. Such a simplification is of great help in the examination of the general nature of the instability.

The Generalized Wing-Bending Coordinate

Before the generalized bending coordinate can be established, a brief look at the nature of the fundamental, uncoupled, free-free, wing-bending mode (in vacuo) is necessary. Consider an airplane with large concentrated wing-tip masses oscillating in such a mode. If the generalized wing-bending coordinate at any time is called y, and the corresponding mode shape is called $a(\eta)$, the vertical position of the wing relative to the node at any span station η is $ya(\eta)$ (fig. 1). The mode shape $a(\eta)$ may be considered to be made up of two parts

$$a(\eta) = a_0(\eta) + a(0)$$

where $a_0(\eta)$ is simply the mode shape referenced to the wing root rather than the node (fig. 2). With this definition and with $a_0(\eta)$ normalized to 1.0 at the wing tip, it is evident that y is the cantilever wing-tip deflection (see fig. 1). The quantity $a(0)$ can be determined from the equilibrium requirement for the freely oscillating system in the absence of aerodynamic forces

$$\int_{-1}^{1} \mu(\eta) \frac{d^2}{dt^2} \left[ya(\eta)\right] d\eta = \ddot{y} \int_{-1}^{1} \mu(\eta) a(\eta) d\eta = 0$$

where $\mu(\eta)$ is the spanwise mass distribution including the concentrated masses. Because the mode is symmetric the integration need only be over the semispan. Substituting $a(\eta) = a_o(\eta) + a(0)$ and dividing the equation by $\ddot{y}$ yield

$$2\int_o^1 a\mu \, d\eta = 2\int_o^1 a_o\mu \, d\eta + 2a(0)\int_o^1 \mu \, d\eta = 0$$

or

$$2\int_o^1 a_o\mu \, d\eta + a(0)M = 0$$

where M is the mass of the airplane. Then

$$a(\eta) = a_o(\eta) - \frac{m}{M} \tag{1}$$

where

$$m = 2\int_o^1 a_o\mu \, d\eta$$

It should be noticed that if the distributed mass in the wings were considered negligible, m would simply be the sum of both concentrated wing-tip masses. (Note in fig. 2 that $a_o(0) = 0$, excluding the fuselage mass, and $a_o(1) = 1$.) Now if $a_o(\eta)$ is assumed to remain unchanged, $a(\eta)$ changes with m/M only as shown in equation (1), greatly simplifying the use of a free-free mode as a degree of freedom. Fortunately the present analysis is fairly insensitive to small changes in $a_o(\eta)$, and this assumption has little effect on the results. The reason for this will become evident later.

The generalized wing-bending coordinate, then, will be represented by the cantilever wing-tip deflection y, where a value of y implies a spanwise deflection relative to the node of $y\,(a_o(\eta) - m/M)$.

Kinetic Energy

The kinetic energy of the two degree of freedom system is $(1/2)\int v^2 dM$ where v is the local velocity in space at the location of the differential mass dM and the integration is made over the whole airplane. Small angles being assumed, the local velocity may be expressed in terms of the two coordinates and can be expressed as

$$v = \dot{\theta}x - \dot{y}a(\eta)$$

where x is the longitudinal distance from the airplane center of gravity, positive forward. Then

$$KE = \frac{1}{2} \int_{\text{airplane}} \left[\dot{\theta}^2 x^2 - 2\dot{\theta}x\dot{y}a(\eta) + \dot{y}^2 a(\eta)^2 \right] dM$$

$$= \frac{1}{2} \dot{\theta}^2 I - 2\dot{y}\dot{\theta} \int_0^1 sa \, d\eta + \dot{y}^2 \int_0^1 \mu a^2 d\eta$$

where I is total pitching moment of inertia about the airplane center of gravity and $s(\eta)$ is the spanwise distribution of static mass moment about the airplane center of gravity. Note that $\int_0^1 sa \, d\eta = \int_0^1 sa_o d\eta$ since $\int_0^1 s \, d\eta = 0$. Thus, letting

$$x_p = \frac{\int_0^1 sa_o d\eta}{\int_0^1 \mu a_o d\eta}$$

$$m_g = 2 \int_0^1 a^2 \mu \, d\eta$$

and remembering that $m = 2 \int_0^1 a_o \mu \, d\eta$

$$KE = \frac{1}{2} \dot{\theta}^2 I - \dot{y}\dot{\theta} x_p m + \frac{1}{2} \dot{y}^2 m_g$$

When the distributed mass of the wing is considered negligible, x_p simply becomes the longitudinal distance between the center of gravity of the concentrated wing-tip mass and the airplane center of gravity.

Potential Energy

The only potential energy in the system is the strain energy in the wing. Since $a_o(\eta)$ is held constant the strain energy is a function of y only and can be written

$$PE = \frac{1}{2} K_y y^2$$

where K_y is an effective spring constant. In terms of the uncoupled, free-free, natural bending frequency ω_y, K_y can be written as $m_g\omega_y^2$. The bending shape is very critical in the determination of K_y; but, as will be seen, this problem is bypassed in the method to be presented.

Lagrange's Equations

The two simultaneous equations of motion are obtained from Lagrange's equation by substituting the expressions for kinetic and potential energy with the coordinates y and θ.

$$\left.\begin{aligned} \frac{d}{dt}\left(\frac{\partial KE}{\partial \dot{\theta}}\right) + \frac{\partial PE}{\partial \theta} &= Q_1 \\ \frac{d}{dt}\left(\frac{\partial KE}{\partial \dot{y}}\right) + \frac{\partial PE}{\partial y} &= Q_2 \end{aligned}\right\} \tag{2}$$

where $\partial PE/\partial\theta$ happens to be zero. The Q's are the generalized aerodynamic forces. Structural damping is neglected. When the indicated differentiations are performed, the equations become

$$I\ddot{\theta} - mx_p\ddot{y} = Q_1 \tag{3a}$$

$$-mx_p\ddot{\theta} + m_g\ddot{y} + K_y y = Q_2 \tag{3b}$$

Generalized Aerodynamic Forces

A generalized force is the work done per unit displacement when the system undergoes a virtual displacement of one of the degrees of freedom. The generalized aerodynamic force is assumed to be composed of terms which are linearly dependent on y, θ, and their derivatives with respect to time. If unsteady aerodynamics are neglected, the essential components of the generalized forces for a straight-winged airplane can be written

$$Q_1 = M_{\dot{\theta}}\dot{\theta} + M_\theta\theta - \left(2\int_0^1 \frac{l_a}{V}\, x_{ac}\, d\eta\right)\dot{y}$$

$$Q_2 = \left(2\int_0^1 a l_\theta\, d\eta\right)\theta + \left(2\int_0^1 a\,\frac{l_a}{V}\, d\eta\right)\dot{y}$$

where a term is positive if the force or moment involved is directed in the positive direction of the appropriate coordinate. The derivatives $M_{\dot{\theta}}$ and M_θ can be readily written in terms of the conventional airplane stability derivatives.

$$M_{\dot{\theta}} = qS\bar{c}(C_{m_q} + C_{m_{\dot{\alpha}}}) , \qquad M_{\theta} = qS\bar{c}C_{m_{\alpha}}$$

The term $l_a(\eta)$ can be interpreted as the air load distribution resulting from a spanwise angle-of-attack distribution defined by $a(\eta)$ in radians, and $l_\theta(\eta)$ can be interpreted as the air load distribution resulting from a uniform angle-of-attack distribution of 1 radian. The generalized bending force due to $\dot{\theta}$ and pitching moment due to $\ddot{y}$ (from downwash lag) were considered negligible.

The air load distribution l_a can be written as the combination of the loading caused by an angle-of-attack distribution of $a_o(\eta)$ radians and $(m/M)l_\theta$ or

$$l_a = l_{a_o} - \frac{m}{M} l_\theta$$

The advantage of this approach is that the generalized aerodynamic forces can be written as explicit functions of m/M. If this relation and the fact that $a(\eta) = a_o(\eta) - (m/M)$ are used, the expressions of Q_1 and Q_2 may be rewritten

$$Q_1 = M_{\dot{\theta}}\dot{\theta} + M_\theta\theta - \frac{1}{V}\left(x_a 2\int_o^1 l_{a_o}d\eta - \frac{m}{M} 2\int_o^1 l_\theta x_{ac}d\eta\right)\dot{y}$$

$$Q_2 = \left(2\int_o^1 a_o l_\theta d\eta - \frac{m}{M} 2\int_o^1 l_\theta d\eta\right)\theta +$$

$$\frac{1}{V}\left[2\int_o^1 a_o l_{a_o}d\eta - \frac{m}{M}\left(2\int_o^1 a_o l_\theta d\eta + 2\int_o^1 l_{a_o}d\eta\right) + \left(\frac{m}{M}\right)^2 2\int_o^1 l_\theta d\eta\right]\dot{y}$$

where the constant x_a in Q_1 results from the fact that l_{a_o} contains no tail or fuselage effect and the assumption that x_a is uniform over the span. For convenience all the terms involving spanwise integrations will be designated as aerodynamic derivatives represented by single symbols with subscripts.

$$Q_1 = M_{\dot{\theta}}\dot{\theta} + M_\theta\theta - \frac{1}{V}\left(x_a Z_{a_o} + \frac{m}{M} M_\theta\right)\dot{y} \tag{4a}$$

$$Q_2 = \left(Y_\theta - \frac{m}{M} Z_\theta\right)\theta + \frac{1}{V}\left[Y_{a_o} - \frac{m}{M}\left(Y_\theta + Z_{a_o}\right) + \left(\frac{m}{M}\right)^2 Z_\theta\right]\dot{y} \tag{4b}$$

The term Z_θ is the rate of change of vertical force with θ and can be written in terms of the familiar airplane lift curve slope as $Z_\theta = -qSC_{L_\alpha}$; Z_{a_o} is the rate of change of vertical force caused by an angle-of-attack distribution $(\dot{y}/V)a_o(\eta)$ with $\dot{y}/V$; Y_θ and Y_{a_o} are

generalized wing-bending force derivatives whose definitions follow from the subscripts. Small changes in $a_o(\eta)$ have been found to have little effect on these derivatives.

Equations of Motion

If equations (3) and (4) are combined a set of homogeneous equations of motion can be written. With D as the differential operator d/dt, these equations are

$$\left(ID^2 - M_{\dot{\theta}}D - M_\theta\right)\theta + \left[-mx_pD^2 + \frac{1}{V}\left(\frac{m}{M}M_\theta + x_aZ_{a_o}\right)D\right]y = 0 \tag{5a}$$

$$\left[-mx_pD^2 - \left(Y_\theta - \frac{m}{M}Z_\theta\right)\right]\theta + \left\{m_gD^2 - \frac{1}{V}\left[Y_{a_o} - \frac{m}{M}\left(Y_\theta + Z_{a_o}\right) + \left(\frac{m}{M}\right)^2 Z_\theta\right]D + K_y\right\}y = 0 \tag{5b}$$

These equations will be useful in the examination of the wing-bending mode but, since no independent vertical translation of the airplane is allowed, the airplane short-period mode is not well represented. In the development of the equations the coordinate deflections are held to small displacements, unsteady aerodynamics are not included, and a constant bending shape $a_o(\eta)$ is assumed.

DETERMINATION OF STABILITY BOUNDARIES

Dimensionless Form of Equations of Motion

The reduction of the equations of motion to the two degree of freedom form of equations (5) makes possible an analysis in general algebraic terms of any airplane to which the equations are applicable. For a general study it is convenient to group the variable quantities describing the airplane characteristics and flight conditions into dimensionless parameters.

In the analysis of equations (5) the following dimensionless quantities were found to be convenient:

τ dimensionless time, $\omega_\theta t$

m' effective tip mass ratio, $\frac{m}{M}$

k_θ dimensionless frequency in uncoupled pitch, $\frac{r\omega_\theta}{V}$

ζ_θ damping ratio of airplane in uncoupled pitch, $\frac{1}{2}\frac{\omega_\theta M_{\dot\theta}}{M_\theta} = \frac{1}{2}\frac{M_{\dot\theta}}{\omega_\theta I}$

x'_p dimensionless effective tip mass center-of-gravity location, $\frac{x_p}{r}$

x'_a dimensionless wing center-of-pressure location, $\frac{x_a}{r}$

u' dimensionless stability margin, $\frac{M_\theta}{rZ_\theta}$

m'_g generalized wing mass ratio, $\frac{m_g}{M}$

Z'_{a_o} $\frac{Z_{a_o}}{Z_\theta}$

Y'_θ $\frac{Y_\theta}{Z_\theta}$

Y'_{a_o} $\frac{Y_{a_o}}{Z_\theta}$

In terms of these new quantities equations (5) become

$$p^2\theta + 2\zeta_\theta d\theta + \theta - m'x'_p p^2\left(\frac{y}{r}\right) - k_\theta\left(m' + \frac{x_a}{u} Z'_{a_o}\right)p\left(\frac{y}{r}\right) = 0 \tag{6a}$$

$$-\frac{m'x'_p}{m'_g} p^2\theta + \frac{1}{u'm'_g}(Y'_\theta - m')\theta + p^2\left(\frac{y}{r}\right) + \frac{k_\theta}{m'_g u'}\left[Y'_{a_o} - m'\left(Y'_\theta + Z'_{a_o}\right) + m'^2\right]p\left(\frac{y}{r}\right) + \left(\frac{\omega_y}{\omega_\theta}\right)^2\left(\frac{y}{r}\right) = 0 \tag{6b}$$

where p is a new differential operator meaning $d/d\tau$.

The Criterion for Neutral Stability

The conventional method of determining the boundaries of neutral stability is by the Routhe criterion. However, even with a fairly simple fourth-order system such as this the computations are quite tedious and any physical feeling for the mechanism of the instability is lost. The equation system (6) lends itself very well to another method of determining stability boundaries which is satisfactory for the present analysis. It greatly aids in physical interpretation of the cause of instability, and the computations required are very simple.

The system is assumed to be in a steady undamped oscillation at the coupled natural wing-bending frequency, and the necessary conditions for this undamped oscillation to exist are used to define the stability boundaries. If the coupled natural frequency in wing bending is ω_B, then based on the dimensionless time used in equation (6), the natural bending frequency is ω_B/ω_θ, which will be called Ω.

By assuming an undamped solution to equations (6) of the form $y/r = (y_o/r)e^{i\Omega\tau}$ and substituting this solution into the pitching-moment equation (6a) it is easily shown that

$$\theta = (A + iB)\frac{y_o}{r}e^{i\Omega\tau}$$

where

$$A = -\frac{m'x'_p\Omega^2(1-\Omega^2) + 2k_\theta\left(m' + \frac{x_a}{u}Z'_{a_o}\right)\zeta_\theta\Omega^2}{(1-\Omega^2)^2 + (2\zeta_\theta\Omega)^2}$$

and

$$B = \frac{k_\theta\left(m' + \frac{x_a}{u}Z'_{a_o}\right)\Omega(1-\Omega^2) + 2m'x'_p\zeta_\theta\Omega^3}{(1-\Omega^2)^2 + (2\zeta_\theta\Omega)^2}$$

But since $y/r = (y_o/r)e^{i\Omega\tau}$ and $p(y/r) = i\Omega(y_o/r)e^{i\Omega\tau}$, θ can be written as

$$\theta = A\left(\frac{y}{r}\right) + \frac{B}{\Omega}p\left(\frac{y}{r}\right)$$

and

$$p^2\theta = -\Omega^2\theta$$

Using the expression for θ, the generalized bending force equation (6b) can be written as

$$p^2\left(\frac{y}{r}\right) + \left\{\frac{B\Omega x'_p m'}{m'_g} + \frac{B(Y'_\theta - m')}{\Omega u' m'_g} + \frac{k_\theta}{m'_g u'}\left[Y'_{a_o} - m'\left(Y'_\theta + Z'_{a_o}\right) + m'^2\right]\right\}p\left(\frac{y}{r}\right) +$$

$$\left[\frac{x'_p m' A\Omega^2}{m'_g} + \frac{A}{u' m'_g}(Y'_\theta - m') + \left(\frac{\omega_y}{\omega_\theta}\right)^2\right]\left(\frac{y}{r}\right) = 0 \qquad (7)$$

Since this equation is valid only for the case of undamped oscillations (neutral dynamic stability), the coefficient of $p(y/r)$ must vanish. Thus

$$B\Omega x'_p m' + \frac{B(Y'_\theta - m')}{\Omega u'} + \frac{k_\theta}{u'}\left[Y'_{a_o} - m'\left(Y'_\theta + Z'_{a_o}\right) + m'^2\right] = 0 \qquad (8a)$$

This leaves, in equation (7), for sinusoidal motion

$$\frac{x'_p m' A\Omega^2}{m'_g} + \frac{A}{u' m'_g}(Y'_\theta - m') + \left(\frac{\omega_y}{\omega_\theta}\right)^2 = \Omega^2 \qquad (8b)$$

Equation (8a) defines the stability boundary in terms of Ω rather than ω_y/ω_θ. For design use, ω_y/ω_θ could easily be found in terms of Ω from equation (8b) provided m'_g is known accurately. Only equation (8a) was used in this study and it should be noted that neither m'_g nor ω_y appears in this equation. Hence, K_y does not enter in any fashion and the stiffness problem is bypassed, as mentioned earlier. Such an approach, which does not employ equation (8b) to determine ω_y/ω_θ, would be useful if the analysis were used in conjunction with actual flight test, where the coupled bending frequency ω_B ($\omega_B = \Omega\omega_\theta$) would be measured.

Stability Boundaries

Equation (8a) has been used to plot stability boundaries on a plane of m' versus Ω with all other parameters held constant (figs. 3, 4, and 5). Since the number of independent parameters is large, presentation of boundaries for all possible combinations of these parameters over a range of values would be prohibitive. For this reason only a few combinations are shown to illustrate the general effects of variations in each quantity on the boundary.

In figure 3 the quantities varied are x'_p, k_θ, and u'. For computation of these boundaries the other parameters were held constant at the following values: $\zeta_\theta = 0.35$, $x'_a = 0$, $Y'_\theta = 0.270$, $Z'_{a_o} = 0.255$, $Y'_{a_o} = 0.108$. All these except x'_a are values which were calculated for an example airplane and thought to be typical of a straight-wing airplane with large wing-tip pods. The value of x'_a was chosen partly because of simplifications which accompany the value, and partly because it is well within the range of reasonable values. Effects of variations in these quantities are dealt with later. The values of k_θ and u' were chosen to fall in what was considered the range of interest for airplanes which are most likely to encounter this problem.

The boundaries in figures 4 and 5 are calculated with $x'_p = 0$, mainly because of the great simplification afforded by this value. When

x'_p is zero, the boundaries become independent of k_θ and u' as is seen later. The significance of the range of values of x_a/u used in figure 5 will be discussed in the next section.

DISCUSSION OF STABILITY BOUNDARIES

Mode of Instability

The stability boundaries indicate conditions under which undamped oscillations of the system will occur. Since the system is regarded as having two degrees of freedom, it must be determined whether the neutrally stable mode is what has been called coupled wing bending or a coupled mode which is predominantly pitching. The nature of the neutrally stable mode can be determined quite easily for any particular case by substituting the appropriate natural frequency back into the equations and determining the relation between the pitch and wing-bending coordinates.

It was found that the modes of oscillation associated with the boundaries considered in this study involved a maximum value of the ratio $r|\theta|/|y|$ which was on the order of k_θ or, in this study, 0.1. Physically, this means that a point on the airplane fuselage a longitudinal distance from the airplane center of gravity equal to the radius of gyration would have linear oscillation amplitude with respect to the center of gravity, caused by pitching, usually less than one-tenth the oscillation amplitude of the wing tip referred to the center of gravity. From this observation it can be said that the coupled mode associated with the boundaries is primarily one of wing bending. (The largest pitching amplitudes occur under conditions of large longitudinal displacements of the tip mass center of gravity from the airplane center of gravity and the higher frequency ratios.)

The phasing of pitch with respect to cantilever bending deflection in these neutrally stable modes (except for one boundary discussed later) is such that θ leads y by an amount ranging from a fairly small angle to something greater than 90° (vector plot, sketch (a)). The larger lead angles are associated with small values of Ω and the smaller lead angles with values of Ω near 1.0. Physically this phase relation means that when the wing tip is traveling downward with maximum velocity during the undamped oscillation (at zero displacement), the pitch angle is positive. In other words, there is a positive component of pitch in phase with bending velocity.

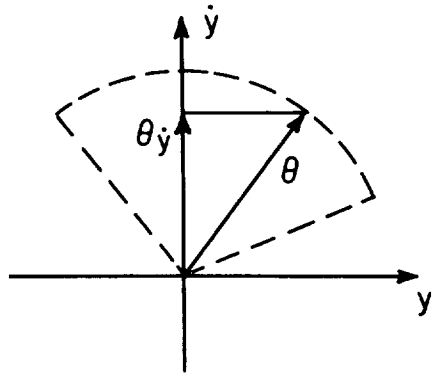

Sketch (a)

It is this in-phase component of pitch which is the major factor in reducing the damping to zero, since the

air loads caused by the in-phase pitch effectively alter those which normally supply the damping in the uncoupled wing-bending mode. This fact can be illustrated with the aid of a rather simplified picture of the air loads which provide the damping. The distribution of vertical velocity along the span, $\dot{y}a(\eta)$, for an airplane with rather large wing-tip masses might appear as in figure 6(a) during a wing-bending oscillation. Such a velocity distribution would have associated with it a spanwise angle-of-attack distribution equal to $(\dot{y}/V)a(\eta)$ (fig. 6(b)) during forward flight and consequently a spanwise loading $(\dot{y}/V)l_a$ which would resemble that in figure 6(c). In an uncoupled bending oscillation or a bending oscillation in which there were no pitch in phase with bending velocity $(\theta_{\dot{y}})$, it is this loading which would tend to damp the oscillation. It can be seen from the figures that such an oscillation would always be stable since the air loads oppose the motion essentially over the entire span.

In the unstable bending modes mentioned above, however, there is a component of airplane pitch in phase with bending velocity which is accompanied, of course, by a spanwise loading similar to that shown in figure 6(d). The effective span loading in phase with $\dot{y}$, which determines the damping, then, becomes the sum of the loadings of figures 6(c) and 6(d) shown in figure 6(e). It is easily seen from a comparison of figure 6(e) with 6(a) that the air load favors rather than opposes the direction of motion of the wing over the center part of the span. Integration of the product of the loading of figure 6(e) with the mode shape $a(\eta)$ over the span indicates whether the net effect is stable, neutrally stable, or unstable oscillation. Again by looking at the figures one can see that the stability of the oscillation as determined from this integration will depend mostly on the amount of pitch in phase with $\dot{y}$ and the spanwise location of the nodes. This latter quantity is determined by the effective tip mass ratio m' and the bending shape. Movement of the nodes toward the tips (or increasing m') and increasing the component of pitch in phase with bending velocity are both contributory to instability in this mode.

A brief look at the stability criterion (eq. (8a)) will help in the physical interpretation of the effects of the various parameters on the stability boundaries. The third term of this expression is simply the discriminant or stability criterion for the uncoupled wing-bending mode (see coefficient of $p(y/r)$ in eq. 6(b)). There is no positive value of m' between 0 and 1 for which the bracketed expression becomes 0 with realistic aerodynamic derivatives, meaning that the single degree of freedom wing-bending system cannot become unstable. This was demonstrated physically above.

The second term of equation (8a) is proportional to the component of pitch in phase with bending velocity since it was shown that $\theta = A(y/r) + (B/\Omega)p(y/r)$ and is the only additional term which would appear in the stability criterion of the coupled system if x'_p were zero. Also, it was found in the calculation of the stability boundaries

that the first term, proportional to pitching acceleration in phase with bending velocity, is not an important contributor for Ω less than 1.0 even when x'_p is not zero, so that the examination of only the second and third terms can give much insight into the behavior of the boundaries at the lower frequency ratios. If the first term is neglected equation (8a) can be rewritten in the following manner:

$$Y'_{a_o} + \frac{B}{\Omega k_\theta} Y'_{\dot{\theta}} - m'\left(Y'_{\dot{\theta}} + Z'_{a_o} + \frac{B}{\Omega k_\theta}\right) + m'^2 = 0 \qquad (9)$$

The term $B/\Omega k_\theta$ can be shown equal to $\theta_{\dot{y}}/(\dot{y}/V)$, where $\theta_{\dot{y}} = (B/\Omega)p(y/r)$ is the component of pitch in phase with bending velocity and $\dot{y}/V$ is simply the characteristic angle of attack caused by wing-bending velocity. As $\theta_{\dot{y}}$ goes to zero equation (9) becomes the same as the third term of equation (8a). The effect of this term is to alter the aerodynamic derivatives as they appear in the third term of equation (8a).

A qualitative plot of m' required for neutral stability versus $\theta_{\dot{y}}/(\dot{y}/V)$ based on the simplified criterion, equation (9), is shown in figure 7. Since all the boundaries in figures 3, 4, and 5 except one are associated with modes of oscillation involving pitch <u>in</u> phase with bending velocity the right-hand boundary will be of most interest. It can be seen that as the in-phase component of pitch is increased from zero, a value is reached where neutral stability can exist for $0 < m' < 1.0$. As $\theta_{\dot{y}}/(\dot{y}/V)$ increases beyond this value, the value of m' required for neutral stability decreases. This figure will be referred to as the effects of the various parameters are discussed.

The general effect of the first term of equation (8a) is to raise the boundaries in figure 3 with positive values of x'_p above what would be found with equation (9) in the region of $\Omega = 1.0$ and above.

Relation of Boundaries to Existing Airplanes

Now that stability boundaries have been established in terms of several dimensionless quantities, it is of interest to know where existing airplane types stand relative to these boundaries. First, orientation on the $m' - \Omega$ plane will be considered. For airplanes with no mass concentrations at the tips, the effective wing-tip mass is quite small compared with the total airplane mass (m' probably less than 0.1), and the fundamental wing-bending frequency is high in comparison with the uncoupled pitching frequency of the airplane. Such airplanes would be below and to the right of the portion of the $m' - \Omega$ plane shown in figures 3 and 4. One possible exception to this might be a flying wing configuration where the total mass is distributed along the wing. In this case m' might be fairly large. (The value of m' for a uniform beam, an extreme example, is about 0.38.)

The addition of concentrated masses to the wing tips tends to move a given airplane upward and to the left on the plot of m' versus Ω, and, as the concentrated wing-tip mass is increased, the trend continues in the same direction toward the unstable regions. However, even airplanes which are now considered to have very large wing-tip pods have insufficient values of effective tip mass ratio m' to reach any of the boundaries shown in figures 3 and 4. To cite a specific example, a fully loaded F-89D, which represents nearly the upper limit in wing-tip mass ratios for current airplanes, could be shown as a point slightly above m' equal to 0.25 and near $\Omega = 1.0$ for a condition of high speed and low altitude.

The location of the boundary itself on the $m' - \Omega$ plane is a function of some quantities which should be related to existing airplanes. The quantities x_p' and u' are fairly straightforward. They are dimensionless on the radius of gyration instead of the more familiar mean aerodynamic chord, but these two characteristic lengths are of similar size. Again using the F-89D as an example, the approximate range of x_p' is from 0.25 to -0.4, and of u' is from nearly 0 to 0.45. The large value of u' is the result of a center-of-pressure shift in the transonic range, and similar values can be expected for airplanes flying supersonically.

The term k_θ is comparable in value to the familiar reduced frequency encountered in the study of classical flutter, the only difference being the use of radius of gyration instead of semichord as the characteristic length. A value of k_θ equal to 0.1 represents almost the upper limit for present-day fighter-type airplanes. The highest values of k_θ would be encountered at low supersonic speeds and low altitudes.

The term x_a' is the distance of the wing aerodynamic center from the airplane center of gravity in fraction of the radius of gyration r. This quantity may be either positive or negative but will usually be less in absolute magnitude than u' for conventional airplanes.

Effects of Tip Mass Center-of-Gravity Movement

Figure 3 indicates the effect of tip mass center-of-gravity movement on the location of the boundary. As the tip mass center of gravity is moved forward of the airplane center of gravity from $x_p' = 0$ to $x_p' = 0.5$, the unstable region expands downward and to the right on the $m' - \Omega$ plane. This is a destabilizing effect in the sense that an airplane on the stable side of the boundary could become unstable with forward movement of the tip mass. Movement of the tip mass center of gravity in a negative, or aft, direction from the airplane center of gravity has the opposite effect. However, the danger of reaching the boundary for negative x_p' with an actual airplane would be very small, so it is not considered. The marked effectiveness of x_p' in moving the boundary suggests that movement of the tip mass center of gravity would be a useful tool for eliminating any problem involving this type of instability.

The effect of forward displacement of the tip mass on the mode of oscillation is to increase the amplitude and lead angle of θ with respect to y by imposing a pitching moment in phase with bending acceleration. This also means that over most of the frequency range forward movement of the tip mass increases the amount of pitch in phase with bending velocity. By referring to figure 7 it can be seen that an increase in $\theta\dot{y}$ tends to lower the value of m' required for neutral stability. This effect is also evident from the physical argument of figure 6 in that a larger loading near the midspan permits the node lines to be farther from the tips for neutral stability.

Effects of k_θ and u'

Unfortunately, the physical significance of independently varying k_θ and u' is not obvious. The term k_θ is one which arises in the nondimensionalization of time and of forces and moments caused by wing-bending velocity. It is the key quantity in determining the local angle of attack at a point on the wing resulting from a given vertical velocity of that point. When the definition of k_θ is rewritten it acquires an interesting meaning which, although somewhat removed from its origin, helps in obtaining a physical feeling for the term.

$$k_\theta = \frac{\omega_\theta r}{V} = \sqrt{-\frac{M_\theta}{MV^2}}$$

The ratio under the radical in the right-hand expression may be thought of as a ratio of energies. Except for a factor of 2, the denominator is simply the kinetic energy of the airplane due to forward motion, and the numerator can be interpreted as the potential energy resulting from a unit deflection in pitch or the energy contained in an uncoupled, undamped pitching oscillation of unit amplitude. Thus the term becomes a measure of the energy contained in the uncoupled pitching mode as compared to the kinetic energy of the airplane in forward motion.

The definition of u' is very simple but the way in which it enters the problem independent of k_θ is not at all obvious. Just as k_θ, u' can be rewritten to have a physical interpretation quite apart from that of a dimensionless static stability margin. The term u' can be written

$$u' = -\frac{M\omega_\theta^2 r}{Z_\theta}$$

The numerator might be called a characteristics inertia force which would occur during an undamped, uncoupled pitching oscillation of unit amplitude, and the denominator is the corresponding characteristic aerodynamic force on which all aerodynamic forces have been nondimensionalized. With this

interpretation u' becomes a measure of the relative importance of inertia and aerodynamic forces. For example, an independent decrease in u' indicates an increase in the significance of aerodynamic forces in the system. (This can also be seen in eqs. (6).)

The first point of interest is that when $x_p' = 0$, the boundary of figure 3 is independent of k_θ and u'. The reason is that under this condition the coupling between pitch and wing bending is purely aerodynamic. In the more general case when x_p' is not zero, both inertial and aerodynamic coupling occur.

In the range of values considered for x_p' and u', k_θ appeared to have only small effect on the location of the boundaries. The small change that was noticed indicates that an independent increase in k_θ (u' constant) tends to move the boundary upward and to the left on the $m' - \Omega$ plane for positive values of x_p', a favorable direction. It should be remembered that this observation is based only on small values of k_θ. For a given airplane k_θ can be changed significantly only through Mach number effects or change of altitude (or automatic controls).

The effect of changes in u' on the boundaries is seen to be particularly noticeable for values of Ω above 1.0. An independent increase in u' tends to shrink the boundary to the left for positive x_p'. For a given airplane u' can be varied significantly only through Mach number effects (or automatic controls).

Both k_θ and u' are quantities which are determined by considerations other than wing-bending stability, and for this reason could not generally be altered for the purpose of improving the wing-bending characteristics.

Effects of Pitch Damping

It should be remembered that the boundaries in figure 3 were calculated with ζ_θ and x_a/u, and with the aerodynamic derivatives held constant. At this point some of the effects on the boundaries of deviations of ζ_θ and x_a from their assigned values will be examined. These effects will be observed quantitatively only for the condition when $x_p' = 0$, since under this condition the boundaries become independent of k_θ and u', and the stability criterion becomes exactly that of equation (9). These results can be extended qualitatively to other conditions.

The effect on the boundary of changes in pitch damping is illustrated in figure 4. The boundary for $\zeta_\theta = 0.35$ is the same as that for $x_p' = 0$ in figure 3, and the second boundary differs only in that ζ_θ has been lowered to 0.2. The effect of lowering ζ_θ is to extend the unstable region slightly as Ω approaches 1.0. Physically the effect of lowering ζ_θ is to increase the magnitude of pitch in the coupled mode near

$\Omega = 1.0$ through the phenomenon of resonance. This in turn increases the component of pitch in phase with bending velocity and hence the boundary is lowered. This general effect is also present where x_p' is not equal to zero.

Effects of Wing Aerodynamic Center Location

The longitudinal position of the wing aerodynamic center x_a enters into the stability criterion (eq. (8a)) as a ratio x_a/u. Aerodynamically the static stability term M_θ is composed of two major parts, the contribution of the horizontal tail and the contribution of the wing. The wing contribution can be either stabilizing or destabilizing depending on whether the wing aerodynamic center is aft or forward of the airplane center of gravity. The ratio x_a/u is a measure of the contribution of the wing to the total longitudinal static stability M_θ. A positive value indicates a destabilizing wing contribution; a negative value indicates a stabilizing wing contribution; and a value of -1.0 indicates that all the stability is contributed by the wing and none by the tail.

The effect of changing the ratio x_a/u on the boundary for $x_p' = 0$ is shown in figure 5. Except for the changes in x_a/u, all conditions are the same as for the $x_p' = 0$ boundary in figure 3. The boundaries for $x_a/u = 0.5$, 0, and -0.5 give an indication of the effect of this parameter for conventional airplanes. If the wing gives a destabilizing contribution to the longitudinal static stability, the boundaries of figure 3 are generally lowered, and the reverse is true for a stabilizing wing contribution. This effect is more pronounced for low values of Ω than for high values, and, in fact, this is the only parameter discussed so far that has varied the location of the boundary at $\Omega = 0$. This will be discussed in the next section.

The actual mechanics of this effect are based on the fact that the tail contribution to static longitudinal stability is most important in producing a pitching moment proportional to and in phase with bending velocity, since the wing contribution tends to be canceled out in the wing-bending oscillation. The increase in $\theta_{\dot{y}}$ caused by an increase in pitching moment in phase with $\dot{y}$, then, lowers the boundary in accordance with the effect shown in figure 7.

As a matter of interest a boundary was computed for $x_a/u = -2.0$. This is a case where twice the total amount of static stability is contributed by the wing, or, in other words, the "tail" has a negative contribution as in a canard configuration. The result of this computation was the lower boundary in figure 5. The mode of oscillation in this case was primarily wing bending as with the other cases, but the

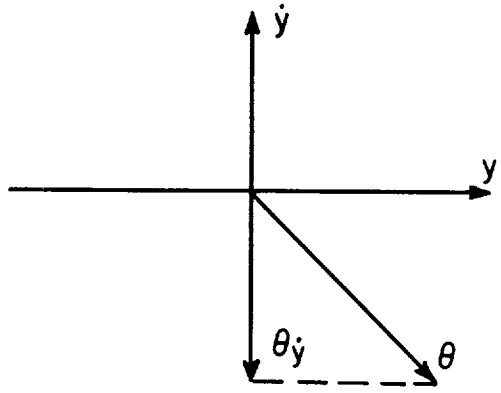

Sketch (b)

pitching motion lagged wing bending, producing a pitch component in antiphase with bending velocity (sketch (b)).

Physically, the canard surface produces a pitching moment in antiphase with bending velocity as opposed to the in-phase pitching moment produced by the conventional tail. As a result of this, a component of pitch in antiphase with wing bending is produced which is large enough to reach the left-hand boundary of figure 7. Also, by reversing the sign of the span loading caused by pitch in phase with $\dot{y}$ in figures 6(d) and 6(e), it is evident that zero damping can be achieved if the nodes are moved inward toward the fuselage (or m' reduced). The possibility of reaching this boundary with an actual airplane is remote because of the unlikely combination of low tip mass ratios m' and low frequency ratios Ω.

Location of Boundaries for Small Ω

For all the boundaries in figures 3 and 4 the value of m' associated with neutral stability was independent of the varying parameters when Ω was very near zero. Letting Ω approach zero in equation (8a) gives the value

$$m' = \frac{Y'_{a_o} + \frac{x_a}{u} Z'_{a_o} Y_{\dot{\theta}}}{Z'_{a_o}\left(1 + \frac{x_a}{u}\right)}$$

Setting x_a/u equal to zero, as was done for figures 3 and 4, reduces the expression to

$$m' = \frac{Y'_{a_o}}{Z'_{a_o}} = \frac{Y_{a_o}}{Z_{a_o}}$$

The location of the boundary for small Ω, then, is dependent only on the aerodynamic derivatives and the ratio x_a/u. For negative values of $x_a/u(> -1)$ the boundary near $\Omega = 0$ is above $m' = Y'_{a_o}/Z'_{a_o}$ and for positive values it is below, as illustrated in figure 5.

When $x_a/u = 0$ the portion of the boundary near $\Omega = 0$ corresponds to the point $(Y_{a_o}/Z_{a_o}, Y_{a_o}/Z_{a_o})$ on the boundary of figure 7. Under this condition calculations indicate that the component of pitch in phase with bending velocity exactly cancels the angle of attack at the fuselage station ($\eta = 0$) resulting from the vertical velocity $-m'\dot{y}/V$. Changes in x_a/u move this point as described earlier.

Knowledge of the behavior of the boundary near $\Omega = 0$ allows qualitative prediction of the effect of changes in Y_{a_o}/Z_{a_o} in this region, a variable not yet considered.

Minimum Value of m' Necessary for Undamped Oscillation

All the boundaries of figures 3, 4, and 5, except the one for the canard configuration in figure 5, were found to correspond to locations on the right-hand boundary in figure 7. It was also mentioned earlier that the combination of parameters necessary to reach the boundary for the canard configuration in figure 5 was a very likely one, and further examination of the stability criterion indicates that almost any combination of parameters necessary to achieve neutral stability on the left-hand boundary of figure 7 is in the same category. For airplanes of more or less conventional configuration then, the right-hand boundary of figure 7 will almost certainly be the critical one.

If only the right-hand boundary is considered, figure 7 shows that undamped oscillations cannot be achieved for values of m' less than Y'_θ, since the boundary approaches this value asymptotically as $\theta_{\dot{y}}$ increases indefinitely. It should be remembered that this was derived with a stability criterion which was useful only for $\Omega < 1.0$, but the minimums of the various boundaries calculated always occurred at values of Ω less than 1.0, so this minimum value of m' is a useful quantity. If m' is below this value, instability by the mechanism considered in this study is very unlikely. Probable values of Y'_θ for a conventional type airplane lie between 0.25 and 0.30.

CONCLUDING REMARKS

An oscillatory instability in wing bending coupled with airplane pitching was examined by means of a simple two degree of freedom representation of a straight-winged airplane. Although many effects were not accounted for, it is felt that the basic mechanism of the instability was well represented in the system. The results should be considered a guide to more detailed analyses for particular cases because of the sacrifice of detail in this study in the interest of generalization. The effects of changes in several quantities describing the airplane and its flight condition on wing-bending stability are shown in the form of stability boundaries.

It was shown that for practical purposes there is a minimum value of the ratio of effective wing-tip mass to total airplane mass below which wing-bending instability cannot occur by this mechanism. It was also found that this instability is most likely to occur under conditions of high ratios of effective tip mass to total airplane mass, ratios of natural coupled wing-bending frequency to natural uncoupled pitching frequency near or below 1.0, and tip mass center-of-gravity locations ahead of the total airplane center of gravity. Movement of the tip mass center-of-gravity location appeared to be the most effective method of avoiding a region of instability for an airplane which is critical in this regard.

Ames Research Center
National Aeronautics and Space Administration
Moffett Field, Calif., Sept. 17, 1958

REFERENCE

1. Cole, Henry A., Jr., and Holleman, Euclid C.: Measured and Predicted Dynamic Response Characteristics of a Flexible Airplane to Elevator Control Over a Frequency Range Including Three Structural Modes. NACA TN 4147, 1958.

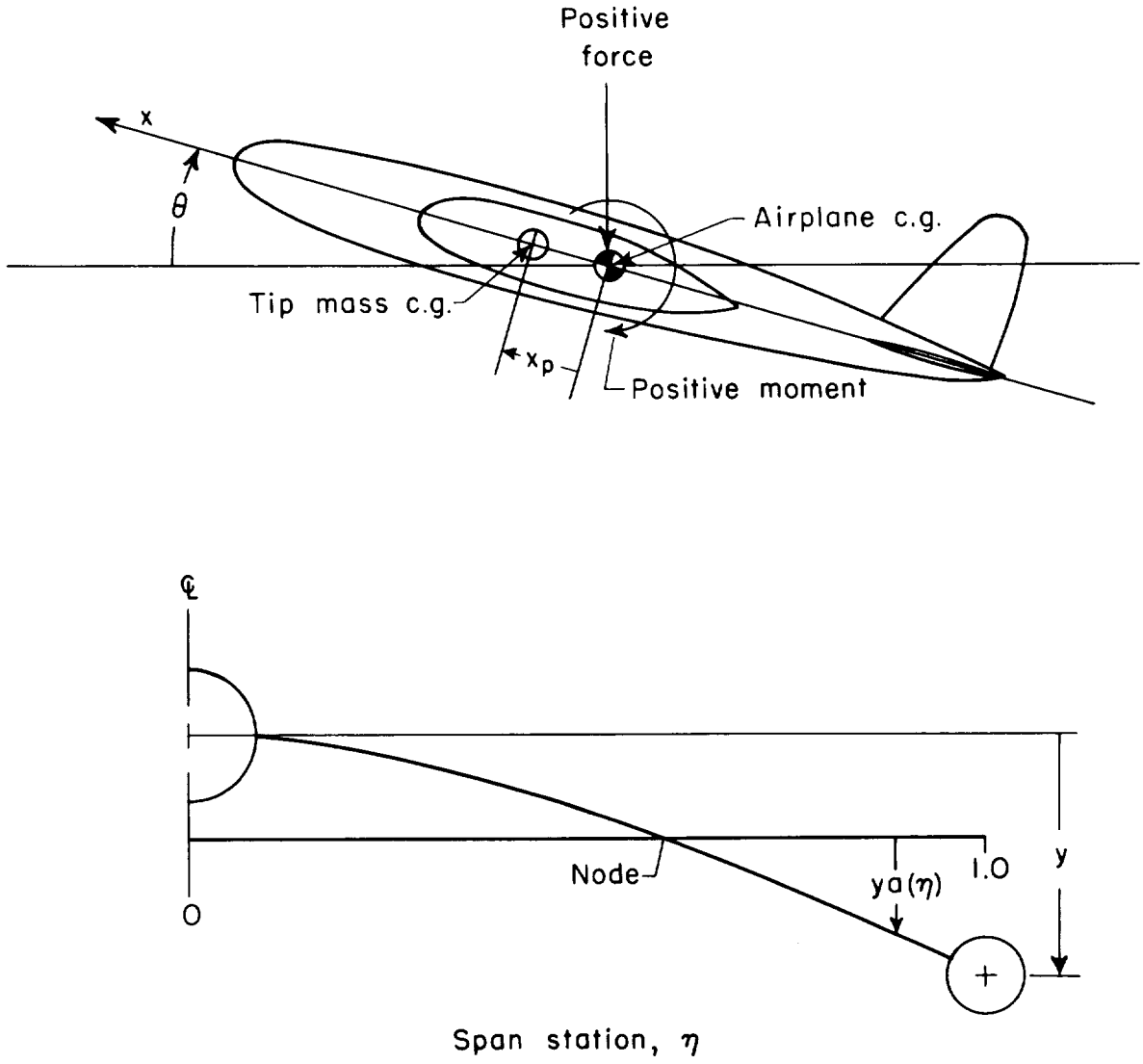

Figure 1.- Pitch and wing-bending coordinates deflected in a positive direction.

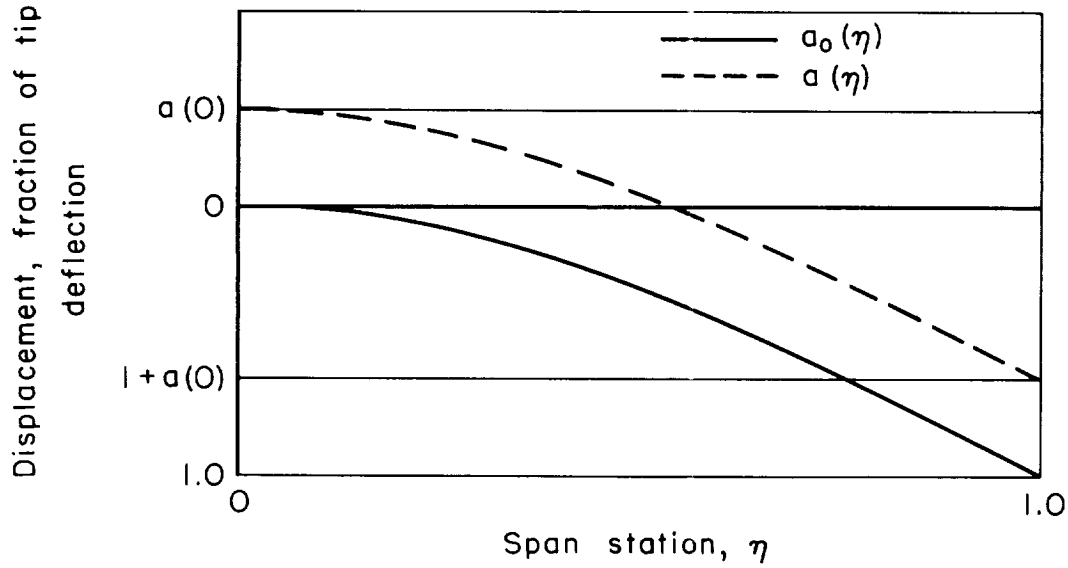

Figure 2.- Uncoupled bending mode shape normalized on cantilever tip deflection; $a_o(\eta)$ referred to root and $\varepsilon(\eta)$ referred to node.

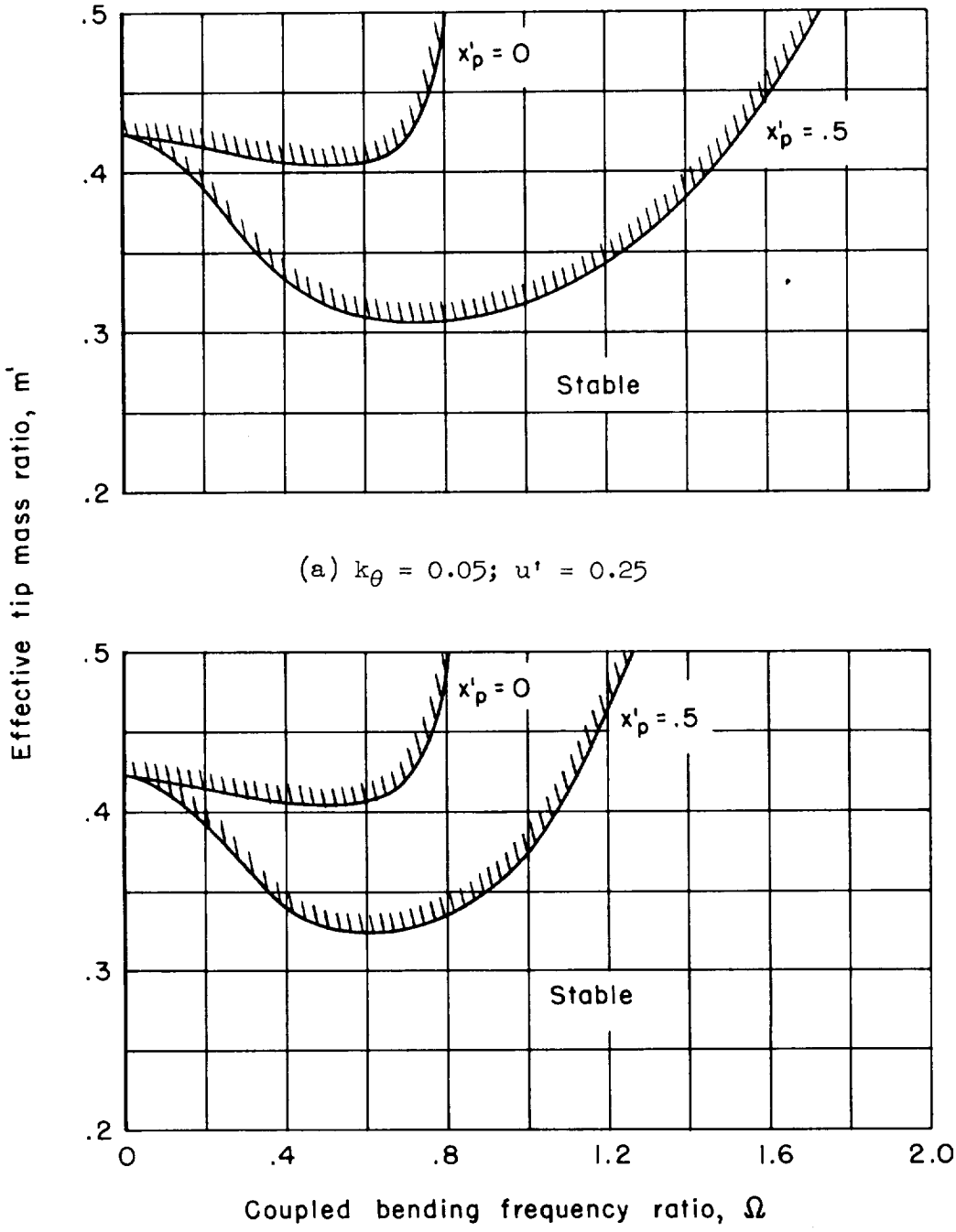

Figure 3.- Effect of tip mass center-of-gravity location on stability boundaries for various values of k_θ and u'; $\zeta_\theta = 0.35$, $x'_a = 0$, $Y'_\theta = 0.270$, $Z'_{a_o} = 0.255$, and $Y'_{a_o} = 0.108$.

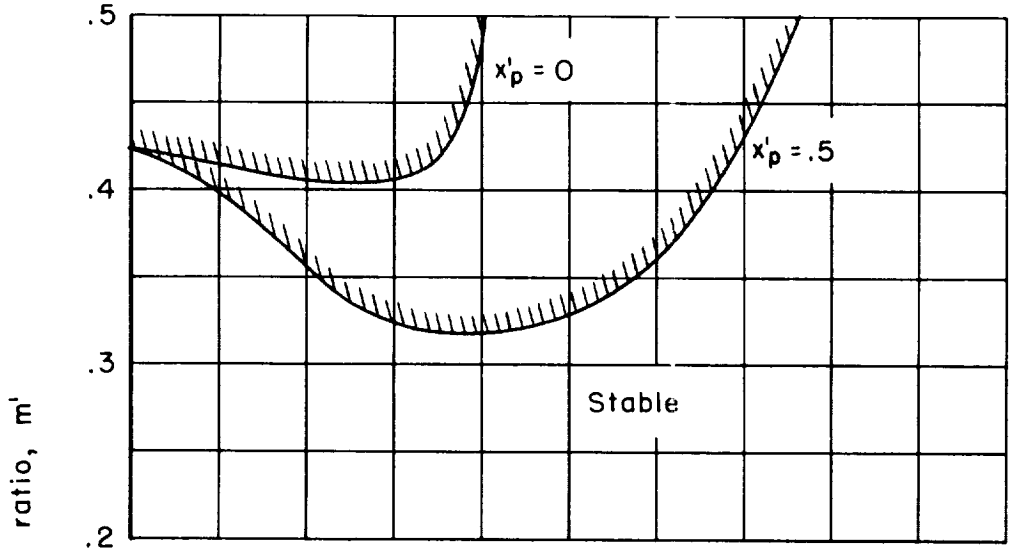

(c) $k_\theta = 0.10$; $u' = 0.25$

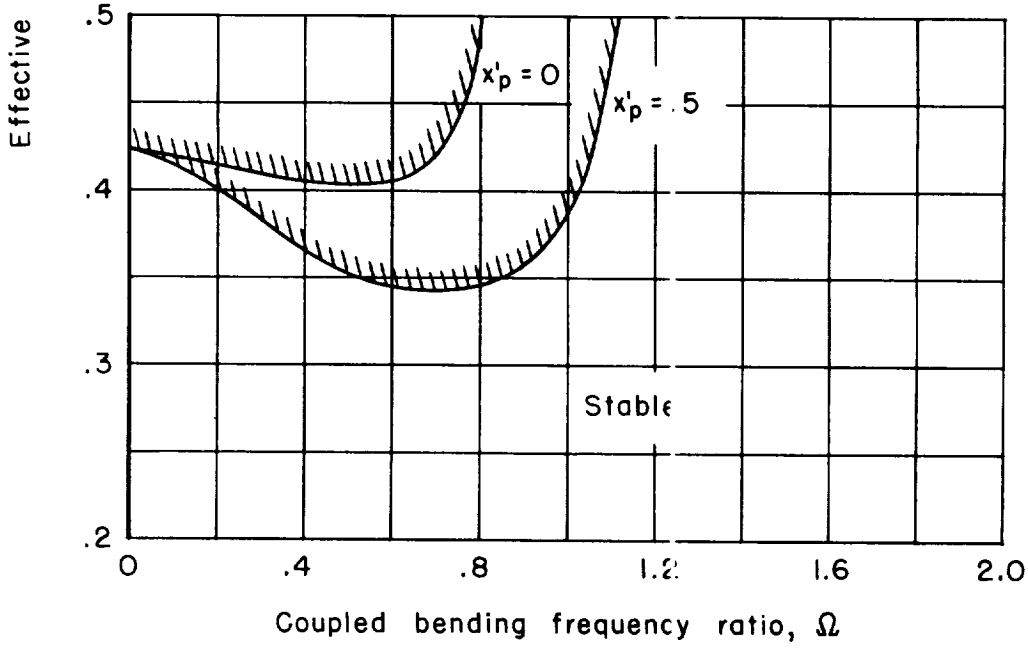

(d) $k_\theta = 0.10$; $u' = 0.50$

Figure 3.- Concluded.

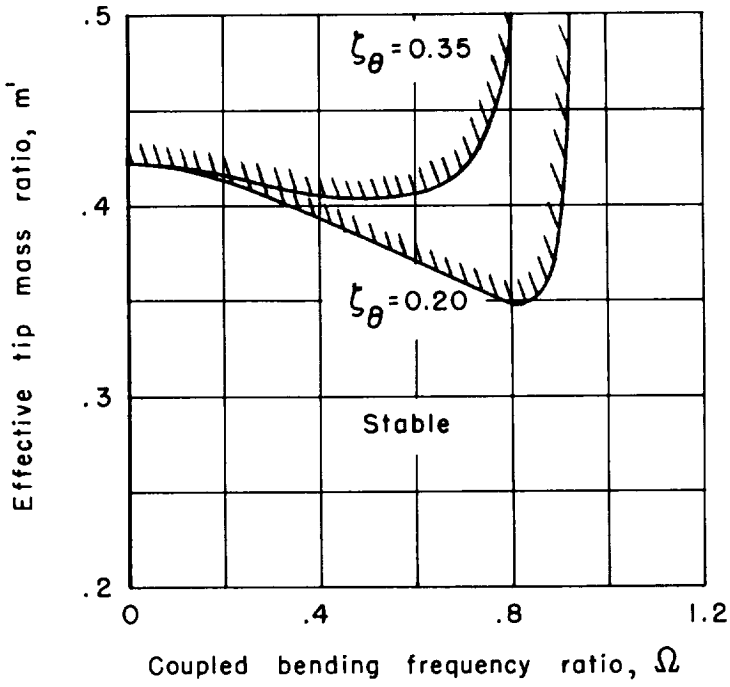

Figure 4.- Effect of pitch damping on stability boundaries; $x'_p = 0$, $x'_a = 0$, $Y'_\theta = 0.270$, $Z'_{a_o} = 0.255$, $Y'_{a_o} = 0.108$.

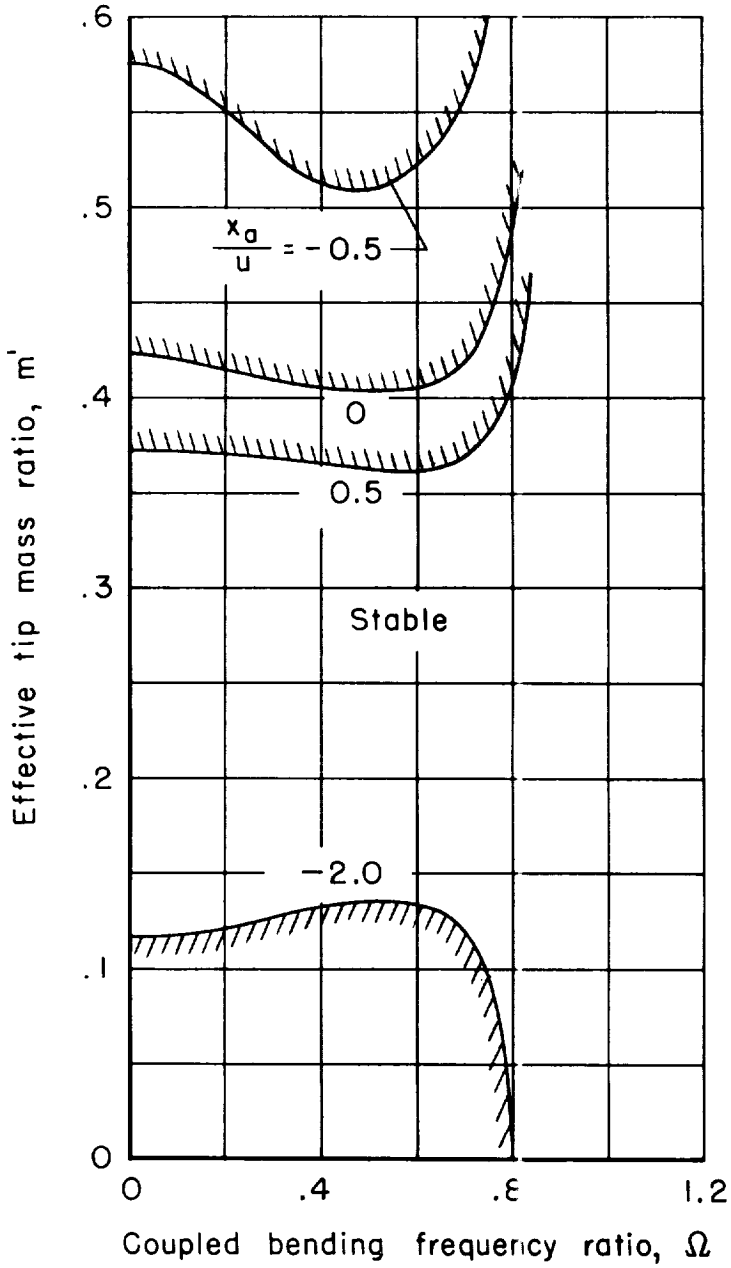

Figure 5.- Effect of wing aerodynamic center location on stability boundaries; $x'_p = 0$, $\zeta_\theta = 0.35$, $Y'_\theta = 0.270$, $Z'_{a_o} = 0.255$, and $Y'_{a_o} = 0.108$.

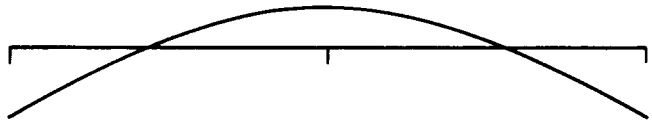

(a) Spanwise vertical velocity distribution, $\dot{y}a(\eta)$.

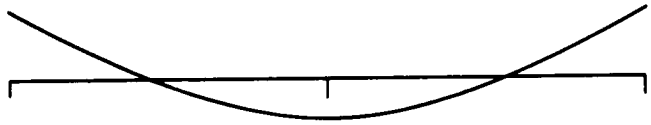

(b) Spanwise angle-of-attack distribution, $\frac{\dot{y}}{V} a(\eta)$.

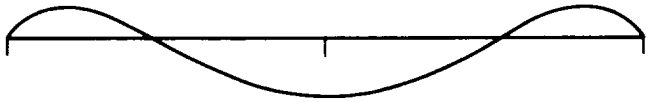

(c) Spanwise air load $\frac{\dot{y}}{V} l_a$ due to angle-of-attack distribution, $\frac{\dot{y}}{V} a(\eta)$.

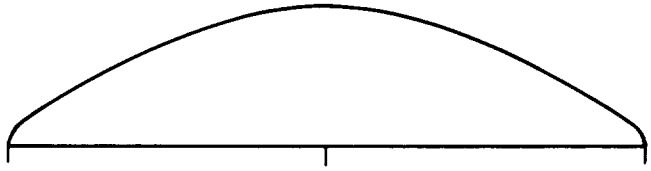

(d) Spanwise air load due to pitch in phase with bending velocity, $\theta_{\dot{y}} l_\theta$.

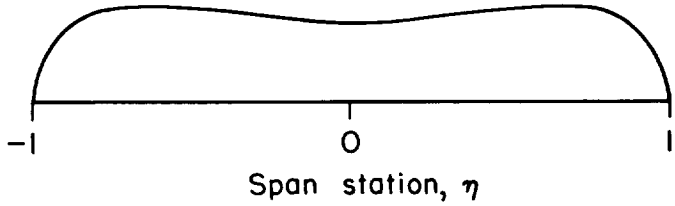

(e) Effective spanwise air load in phase with $\dot{y}$.

Figure 6.- Contributions of wing-bending velocity and airplane pitch to the generalized damping force in the coupled wing-bending mode.

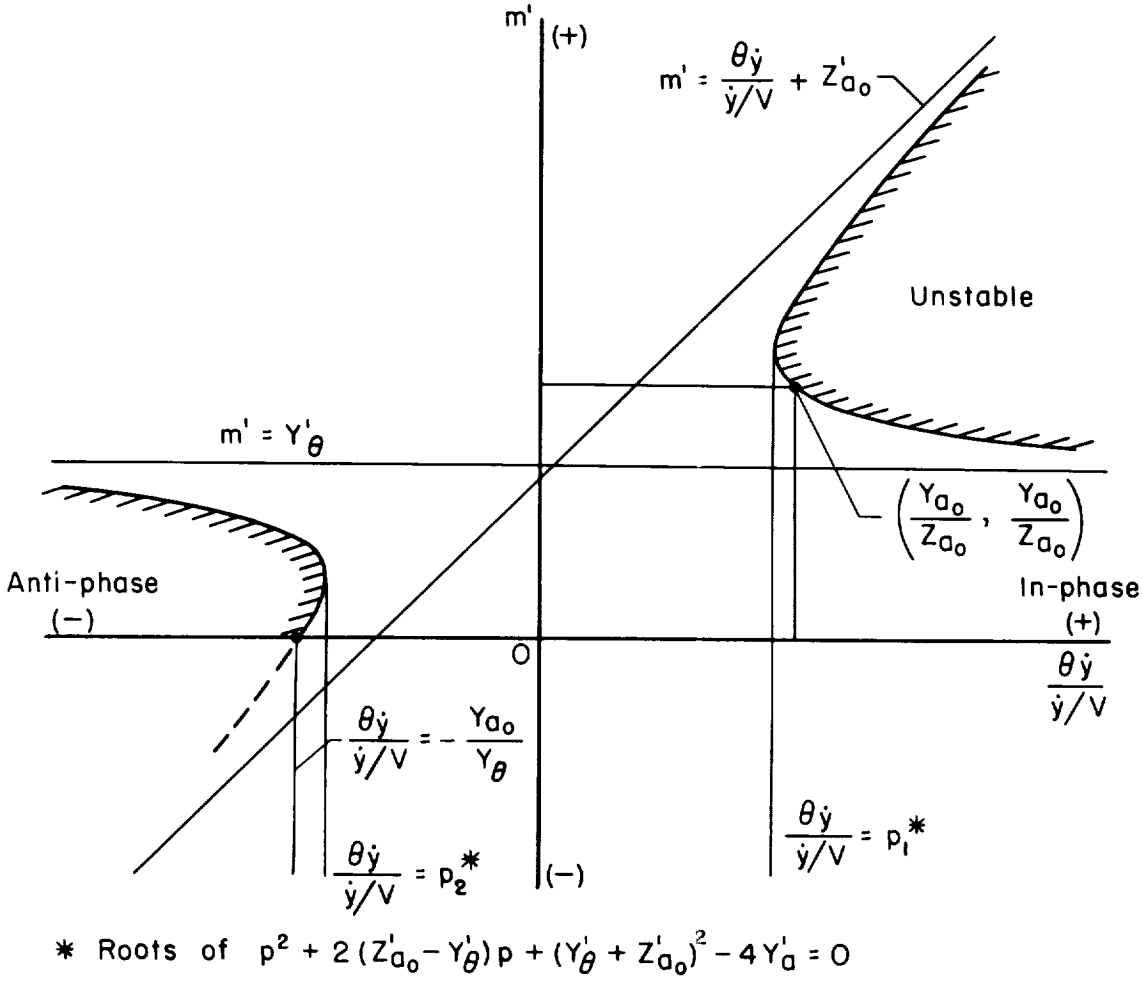

* Roots of $p^2 + 2(Z'_{a_o} - Y'_\theta)p + (Y'_\theta + Z'_{a_o})^2 - 4Y'_a = 0$

Figure 7.- Qualitative stability boundary showing the importance of the component of pitch in phase with bending velocity in determination of wing-bending stability.